CR 167812

E83-10193

AgRISTARS

EW-L3-04394
JSC-18594

Early Warning and Crop Condition Assessment

A Joint Program for Agriculture and Resources Inventory Surveys Through Aerospace Remote Sensing

January 1983

USE OF NOAA-N SATELLITES FOR LAND/WATER DISCRIMINATION AND FLOOD MONITORING

(E83-10193) USE OF NOAA-N SATELLITES FOR LAND/WATER DISCRIMINATION AND FLOOD MONITORING (Lockheed Engineering and Management) 37 p HC A03/MF A01 CSCL 02C N83-20315 Unclas G3/43 00193

G. Tappan
N. C. Horvath
P. C. Doraiswamy

Lockheed Engineering and Management Services Company, Inc.

T. Engman
D. W. Goss

U. S. DEPARTMENT OF AGRICULTURE
1050 Bay Area Boulevard
Houston, Texas 77058

Lyndon B. Johnson Space Center
Houston, Texas 77058

PRECEDING PAGE BLANK NOT FILMED

ORIGINAL PAGE IS OF POOR QUALITY

1. Report No. EW-L3-04394; JSC-18594	2. Government Accession No.	3. Recipient's Catalog No.
4. Title and Subtitle USE OF NOAA-n SATELLITES FOR LAND/WATER DISCRIMINATION AND FLOOD MONITORING		5. Report Date January 1983
		6. Performing Organization Code 26-44
7. Author(s) G. Tappen, N. C. Horvath, P. C. Doraiswamy		8. Performing Organization Report No. LEMSCO-19032
9. Performing Organization Name and Address Lockheed Engineering and Management Services Company, Inc. 1830 NASA Road 1 Houston, Texas 77258		10. Work Unit No.
		11. Contract or Grant No. NAS 9-15800
12. Sponsoring Agency Name and Address Early Warning/Crop Condition Assessment Project Office U. S. Department of Agriculture, 1050 Bay Area Blvd., Houston, Texas 77058 Technical Monitor: V. Whitehead		13. Type of Report and Period Covered Technical Report
		14. Sponsoring Agency Code

15. Supplementary Notes

16. Abstract

A tool for monitoring the extent of major floods has been developed using data collected by the NOAA-6 Advanced Very High Resolution Radiometer (AVHRR). A basic understanding of the spectral returns in AVHRR Channels 1 and 2 for water, soil, and vegetation has been reached using a large number of NOAA-6 scenes from different seasons and geographic locations. A look-up table classifier was developed based on analysis of the reflective channel relationships for each surface feature. The classifier automatically separated land from water and produced classification maps which were registered to a global coordinate system. Testing of the classifier was completed for a number of acquisitions, including coverage of a major flood on the Parana River of Argentina.

17. Key Words (Suggested by Author(s))		18. Distribution Statement	
19. Security Classif. (of this report) Unclassified	20. Security Classif. (of this page) Unclassified	21. No. of Pages	22. Price*

*For sale by the National Technical Information Service, Springfield, Virginia 22161

JSC Form 1424 (Rev Nov 75)

ORIGINAL PAGE IS OF POOR QUALITY

NASA — JSC

ORIGINAL PAGE IS
OF POOR QUALITY

EW-L3-C 394
JSC-18594

USE OF NOAA-n SATELLITES FOR LAND/WATER DISCRIMINATION AND FLOOD MONITORING

Job Order 72-469

Prepared by

G. Tappan
N.C. Horvath
P.C. Doraiswamy

Lockheed Engineering and Management Services Company, Inc.

T. Engman and D. W. Goss

United States Department of Agriculture

APPROVED BY

USDA

G. O. Boatwright, Manager
Early Warning/Crop Condition Assessment Project, AgRISTARS Program

Lockheed-EMSCO

R. F. Hansen, Project Manager
Early Warning Project Office
Inventory Techniques Development Department

LOCKHEED ENGINEERING AND MANAGEMENT SERVICES COMPANY, INC.

Under Contract NAS9-15800

For

Earth Resources Applications Division

Space and Life Sciences Directorate

NATIONAL AERONAUTICS AND SPACE ADMINISTRATION
LYNDON BY. JOHNSON SPACE CENTER
HOUSTON, TEXAS

JANUARY 1983

LEMSCO-19032

V, VI

PREFACE

The Agriculture and Resources Inventory Surveys Through Aerospace Remote Sensing is a multiyear program of research, development, evaluation, and application of aerospace remote sensing for agricultural resources, which began in fiscal year 1980. This program is a cooperative effort of the U.S. Department of Agriculture, the National Aeronautics and Space Administration, the National Oceanic and Atmospheric Administration (U.S. Department of Commerce), the Agency for International Development (U.S. Department of State), and the U.S. Department of the Interior.

PRECEDING PAGE BLANK NOT FILMED

Contents

ABBREVIATIONS

NOAA	National Oceanic and Atmospheric Administration
TIROS	Television Infrared Observation Satellite
AVHRR	Advanced Very High Resolution Radiometer
IMDACS	Integrated Multivariate Data Analysis and Classification System
CRT	Cathode Ray Tube
LAC	Local Area Coverage
Pixel	Picture Element
IJ	A gri system for defining an area of approximately 25 mi. x 25 mi.

COMPUTER PROGRAMS*

LACREG2	Extracts and allocates pixel data to an I,J grid.
LLTOIJ	Locates I,J grid cell latitude and longitude.
FIELDX	Extracts spectral data from the IMDACS files for fields of interest.
FLDMRG	Merges FIELDX generated data into single file.
SCAT	Creates scatter plots and histograms for field data.
SCAT4	Creates scatter plots and histograms of field data in Universal Format with scaling and sun angle corrections
MAP1	Maps a grid cell and classifies data included.
CLASFY	Similar to MAP1 except no map is output.

*See technical manuals JSC-18246 (EW-L2-04312) and JSC-18225 (EW-L2-00741) for further details.

TABLE

FIGURES

1. INTRODUCTION

The NOAA-n satellites of the TIROS series are currently being investigated as potential sources for a variety of earth resources data. Placed in a near-polar, sun-synchronous orbit, their broad field of view permits frequent coverage, making the satellites ideal for monitoring highly dynamic surface phenomena.

The present study is an attempt to utilize NOAA-n Advanced Very High Resolution Radiometer (AVHRR) data as a tool for monitoring the extent of major floods. To realize this, it was necessary to determine the basic spectral characteristics of water bodies and major land cover types as detected by the AVHRR. A large number of NOAA-n scenes from different seasons and different geographic locations were used. From these, many samples of water, soil, and vegetation were selected. The spectral responses of the scenes in the visible and near-infrared wavebands were studied.

A look-up table classifier was developed based on analysis of the channel relationship for each surface feature. The classifier automatically separates land from water and produces classification maps which are registered to a global coordinate system. Testing of the classifier was completed for a number of acquisitions, including coverage of a major flood on the Parana River of Argentina.

The methods of data analysis developed for this project examine large scale phenomena only. Major changes in surface conditions, such as widespread flooding, are the types of situations that these procedures can best distinguish. These broad brush techniques are most useful in a first look at a given event or feature and provide quick views of the general surface conditions.

2. DETERMINING SPECTRAL CHARACTERISTICS OF MAJOR COVER TYPES FROM NOAA-n AVHRR

Initial investigations in determining the use of NOAA-n AVHRR data for monitoring large surface phenomena, such as floods, involved basic analysis of the spectral characteristics of major cover types. While many studies have examined the spectral information content of Landsat data over numerous types of land cover, relatively few have dealt with NOAA-n data. Several significant differences between the NOAA-n and Landsat sensors made it necessary to examine NOAA-n spectral responses to major cover types without relying on results from the wealth of Landsat studies. The major sensor differences between the Landsat and NOAA-n systems are:

1. Slightly different sensitivity ranges in the visible and near-infrared portions of the spectrum,

2. Two to three additional sensors on the NOAA-n satellites, one in the middle-infrared, two in the thermal infrared,

3. Considerable differences in ground resolution (NOAA-n AVHRR ground resolution varies from about 1 x 1 kilometer to 2.5 x 6.5 kilometers, while Landsat MSS sensors provide .056 x .079 kilometers resolution),

4. Large difference in sensor view angle (110.80° for NOAA-n, 11.56° for Landsat), and

5. Difference in the number of digital levels and sensitivities to levels of electromagnetic energy (0-1024 for NOAA-n AVHRR data, 0-127 for the Landsat MSS sensors).

The investigation of the use of NOAA-6 satellite data to assess the areal extent of flooding was initiated with NOAA-6 satellite scenes collected over the central United States by the National Oceanographic and Atmospheric Administration (NOAA). (The images were acquired in 1980 and 1981 spanning the growing season over Texas, Mississippi, Indiana, and Michigan.) The spectral qualities of soil, vegetation, and water were studied. In order to minimize image distortion and large view angle problems, swaths 510 pixels wide centered on nadir were extracted from full scenes 2048 pixels wide. This central swath also corresponded to the optimum ground resolution area of about one square kilometer per pixel.

The images were each displayed on the Integrated Multivariate Data Analysis and Classification System (IMDACS), an interactive image display system which reads the digital spectral data from universal format tapes and converts the digital counts to color intensity levels on a CRT. By using blue and green color guns with the AVHRR channel 1 image, and the red color gun with channel 2, a false-color composite was projected onto the CRT whose hues highly resemble those of standard Landsat color composites. Different types of vegetation cover were represented by various intensities of red, while soils were generally bluish-grey, and water varies from a powdery-blue to black. Detailed comparisons were made between the NOAA-6 color images and the Landsat false color composites of the same areas taken at similar time of year. These comparisons were used to identify and delineate relatively homogeneous areas of agricultural vegetation (e.g., the corn belt of Illinois and Iowa), soil (e.g., land recently plowed for seeding, or arid surfaces lacking significant quantities of green biomass), and water bodies. A total of about sixty sample scenes in the form of rectangular fields were plotted onto the images. The rectangular fields were composed of a range of 50 to over 1,000 pixels, depending upon the size and shape of the area being sampled. These fields represented the three basic cover types: water, soil, and vegetation. The soil and vegetation cover types do not represent perfectly "pure" surfaces since pure cover types rarely exist in nature. However, the samples of these general surface features were closen such that they represented a dominant cover type.

The next major step involved analysis of the spectral data from each sample field. Two methods were used: histograms showing the spectral range and frequency of pixels in each channel, and two-dimensional scatterplots illustrating the feature space location of the three cover types. Figures 2-1, 2-2, and 2-3 show histograms with typical distributions of soil, vegetation, and water pixels. The spectral reflectance of soil in channel

1 (.58-.68um) is somewhat less than its reflectance in channel 2 (.725-1.100). This property of a slight to moderate increase in reflectance from the visible to near-infrared wavelengths is typical of most soils. Figure 2-2 shows responses from a typical sample of healthy agricultural vegetation in channels 1 and 2. The relatively low reflectance level in channel 1 and high level in channel 2 is characteristic of green foliage. The third histogram (Figure 2-3) illustrates the distribution of a sample of water pixels from a lake of moderate turbidity. Because of sediment in the water, the reflectance in channel 1 is somewhat higher than in channel 2, although both are relatively low.

977 PIXELS TOTAL

Reflectance (%)	Channel 1	Channel 2
47	0	0
46	0	0
45	0	0
44	0	0
43	0	0
42	0	0
41	0	0
40	0	0
39	0	0
38	0	0
37	0	0
36	0	0
35	0	0
34	0	0
33	0	0
32	0	0
31	0	0
30	0	0
29	0	0
28	0	0
27	0	0
26	0	0
25	0	0
24	0	0
23	0	0
22	0	1*
21	0	10***
20	0	18****
19	0	20****
18	0	17****
17	0	42******
16	0	49*******
15	3*	108**********
14	9***	92*********
13	31******	145************
12	74**********	197**************
11	64**********	141***********
10	117************	110**********
9	196*****************	25*****
8	230******************	2*
7	215*****************	0
6	16*****	0
5	2*	0
4	0	0
3	0	0
2	0	0
1	0	0
0	0	0

Figure 2-1. Typical soil histogram

```
                          1259 PIXELS TOTAL
                          47     0                                   0
                          46     0                                   0
                          45     0                                   0
                          44     0                                   0
                          43     0                                   0
                          42     0                                   0
                          41     0                                   0
                          40     0                                   0
                          39     0                                   0
                          38     0                                   0
                          37     0                                   0
                          36     0                                   0
                          35     0                                   0
                          34     0                                   0
                          33     0                                   0
                          32     0                                   0
                          31     0                                   0
                          30     0                                   0
                          29     0                                   0
                          28     0                                   0
                          27     0                                   4**
Reflectance               26     0                                  24****
    (%)                   25     0                                  76********
                          24     0                                 179*************
                          23     0                                 411********************
                          22     0                                 351******************
                          21     0                                 171*************
                          20     0                                  40******
                          19     0                                   2*
                          18     0                                   1*
                          17     0                                   0
                          16     0                                   0
                          15     0                                   0
                          14     0                                   0
                          13     0                                   0
                          12     0                                   0
                          11     0                                   0
                          10     3*                                  0
                           9    17****                               0
                           8   139***********                        0
                           7   610************************           0
                           6   490**********************             0
                           5     0                                   0
                           4     0                                   0
                           3     0                                   0
                           2     0                                   0
                           1     0                                   0
                           0     0                                   0

                              Channel 1                          Channel 2
```

Figure 2-2. typical vegetation histogram

174 PIXELS TOTAL

Reflectance (%)	Channel 1	Channel 2
47	0	0
46	0	0
45	0	0
44	0	0
43	0	0
42	0	0
41	0	0
40	0	0
39	0	0
38	0	0
37	0	0
36	0	0
35	0	0
34	0	0
33	0	0
32	0	0
31	0	0
30	0	0
29	0	0
28	0	0
27	0	0
26	0	0
25	0	0
24	0	0
23	0	0
22	0	0
21	0	0
20	0	0
19	0	0
18	0	0
17	0	0
16	0	0
15	0	0
14	0	0
13	0	0
12	0	0
11	0	0
10	0	0
9	0	0
8	0	0
7	0	0
6	18****	0
5	0	2*
4	100**********	16****
3	56*******	56*******
2	0	100**********
1	0	0
0	0	0

Figure 2-3. Typical water histogram

Plots of reflectance in channels 1 and 2 were required for an analysis of the location, size and shape of the three cover types in a two-dimensional feature space. Sample scatterplots of soil, vegetation, and water are presented in Figure 2-4 and the scatterplot code is presented in Table 2-1. These individual plots or clusters show the somewhat limited distribution of particular samples from relatively small areas on the imagery. Since one of the main objectives here was to determine the general responses of these cover types from NOAA-n satellites using a variety of acquisitions, a more relevant analysis of pixel clusters involved a combination of all of the samples of soil, water, and vegetation. These "super" clusters encompassed a much larger range of cover type variations and, as expected, some overlap occurred between classes. Figures 2-5, 2-6, and 2-7 illustrate the three super clusters where the distributions about the class means and distributions are well differentiated. This indicated that automated spectral classification of the three major cover types would perform well. The sixty samples of cover types used in generating the super clusters were quite homogeneous, since the number of outlying pixels around the clusters was small.

Table 2-1. Scatter Plot Code

Code Symbol	Pixel Frequency
1	1
2	2
3	3
4	4
5	5
6	6
7	7
8	8
9	9
A	10-19
B	20-29
C	30-39
D	40-49
E	50-59
F	60-69
G	70-79
H	80-89
I	90-99
J	100-199
K	200-299
L	300-399
M	400-499
N	500-599
O	600-699
P	700-799
Q	800-899
R	900-999
S	1000-1999
T	2000-2999
U	3000-3999
V	4000-4999

W	5000-5999
X	6000-6999
Y	7000-7999
*	9000-00

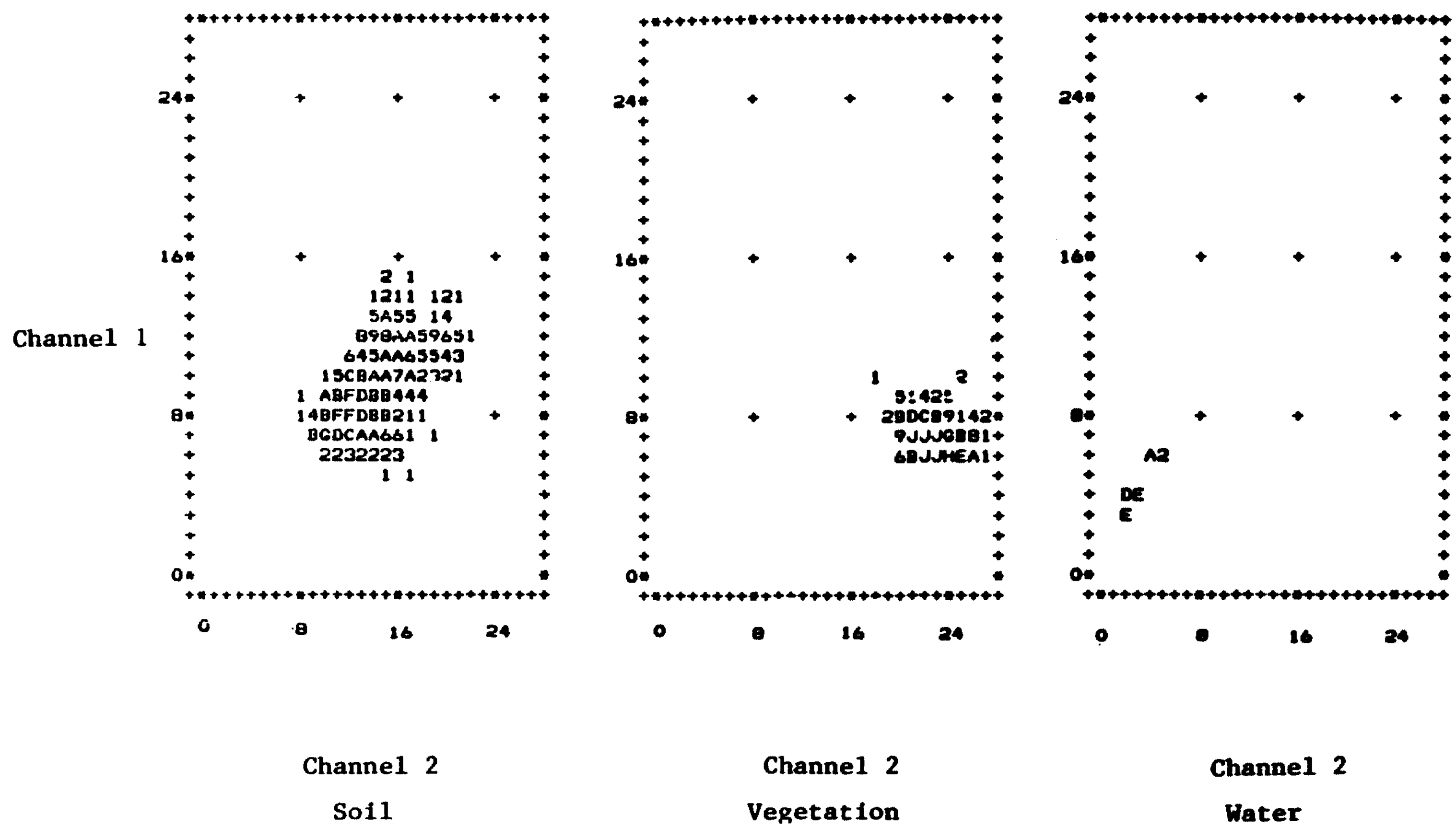

Figure 2-4. Sample plots of soil, vegetation, and water for channels 1 and 2. Channel values are in percent reflectance.

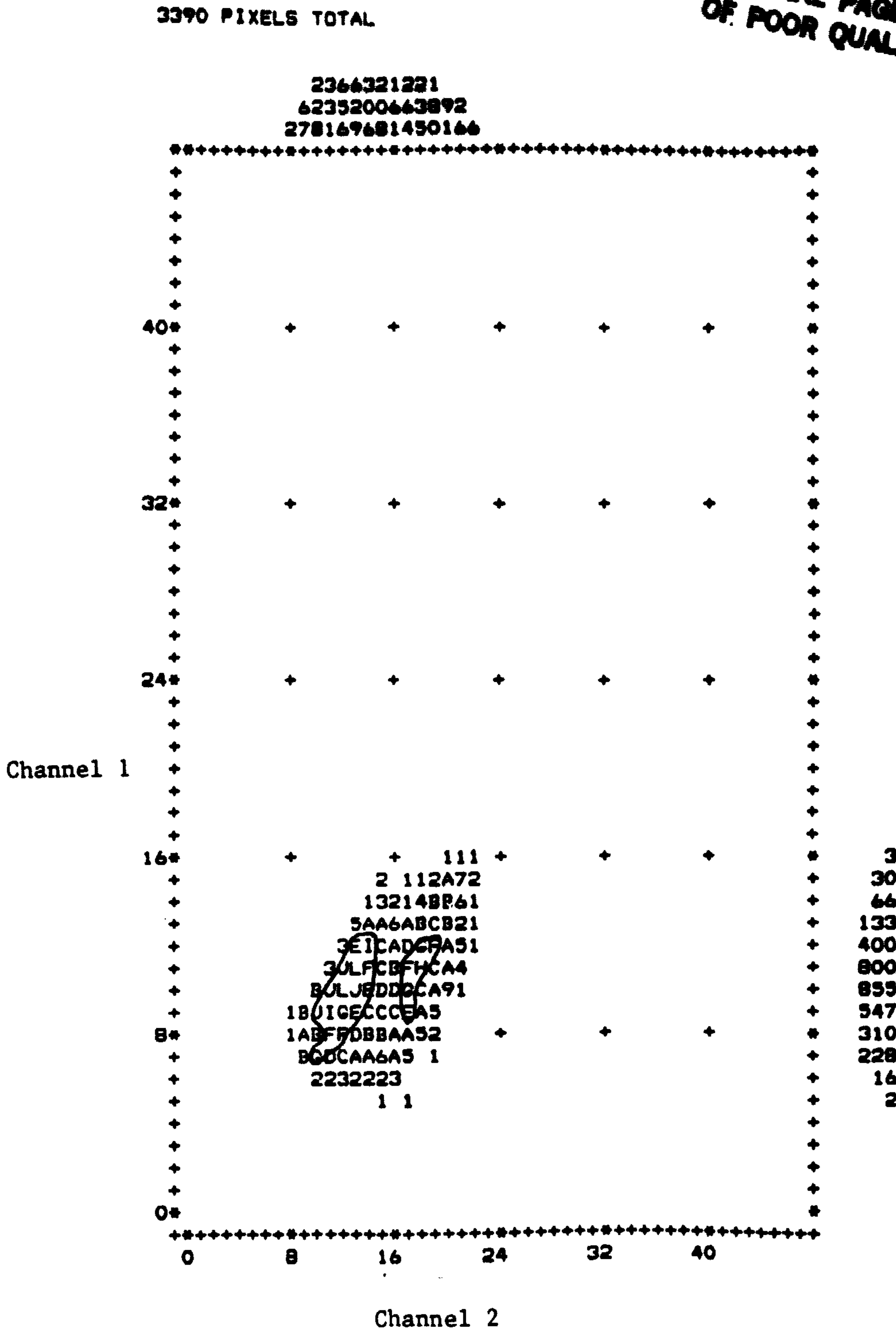

Figure 2-5. Soil super cluster. Percent reflectance values for both channels.

ORIGINAL PAGE IS
OF POOR QUALITY

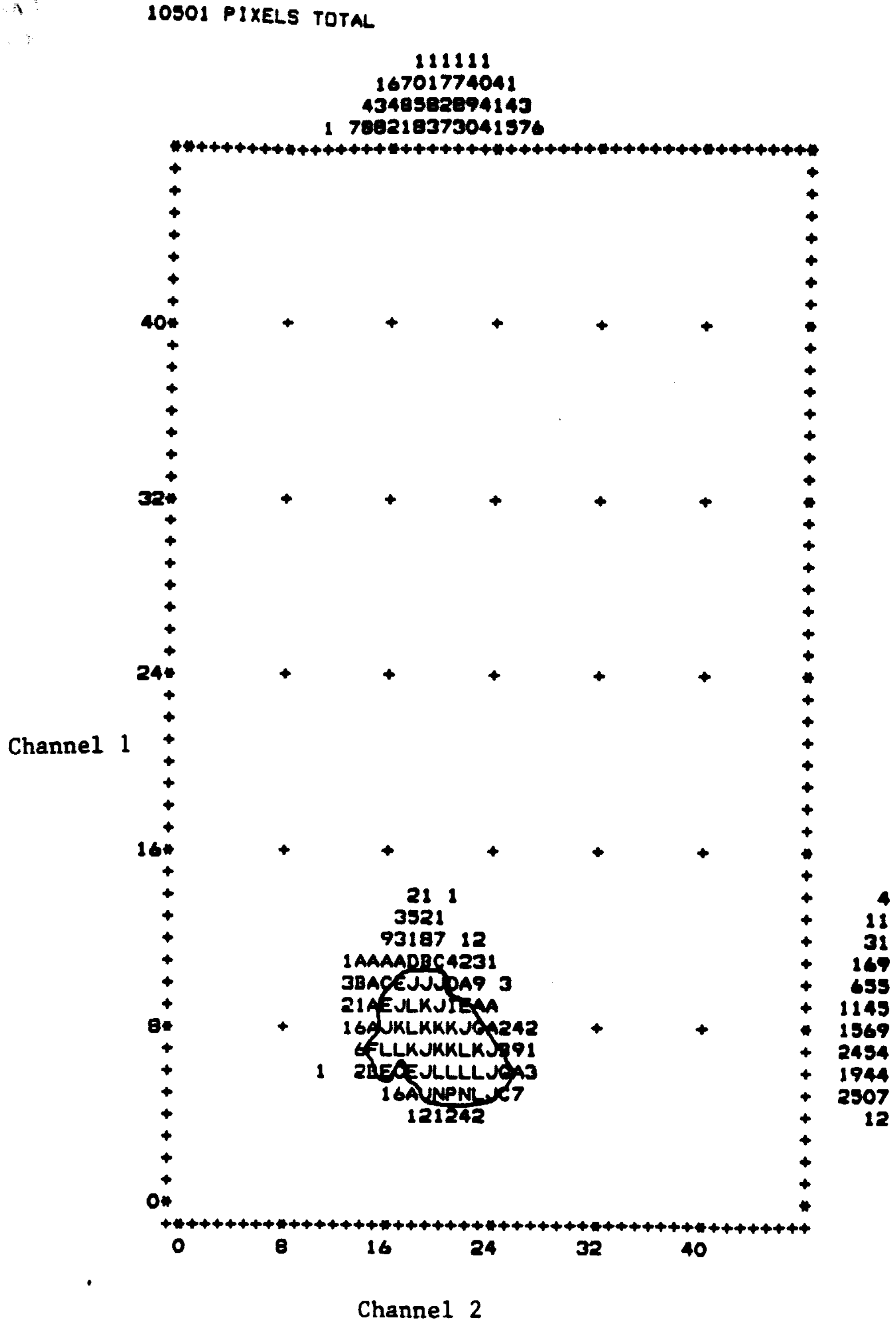

Figure 2-6. Vegetation super cluster. Percent reflectance values for both channels.

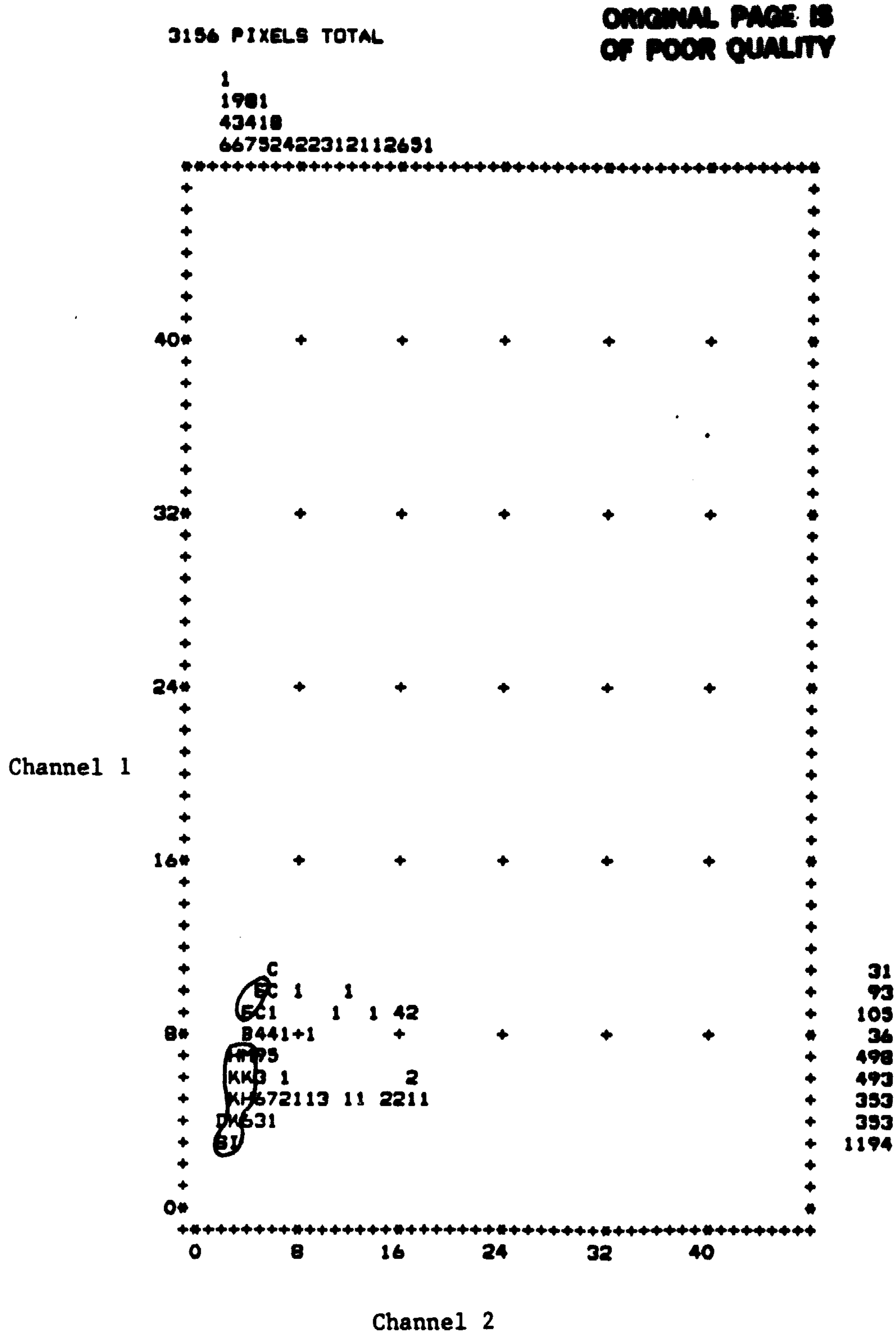

Figure 2-7. Water super cluster. Percent reflectance values for both channels.

3. A LOOK-UP TABLE CLASSIFIER FOR NOAA-n AVHRR DATA

An automated classifier for separating the cover types was developed from the super clusters generated from two channel spectral data. A decision was made to develop a fast, efficient, and straight-forward classifier whose decision boundaries could easily be manipulated. As a result, a form of parallelepiped classifier was designed. Instead of boxing the super clusters into simple rectangular decision regions, a series of small rectangles with stepped boundaries was employed so that the shapes of the pixel clusters would more accurately determine the decision boundaries. Initailly, the decision boundaries were drawn as straight lines defining the decision region of each cluster. In doing so, pixel outliers were ignored, and the decision boundaries were positioned so that they bisected the area of overlap between the soil and vegetation clusters. A solution to the problem was to superimpose a rectangular matrix onto the scatterplot where each matrix cell represents a discrete digital count (percent reflectance) of the AVHRR channel 1 and 2 data. Using the linear boundaries as a guide, the stepped boundaries were drawn along the matrix lines. This defined the decision regions used in the classifier (see Figure 3-1).

The decision logic is in the form of a matrix table to which all pixel values from an image file are compared. A match between the channel values of a given pixel and the values in the matrix assigns the classification category defined in the matrix. This process is repeated for all pixels of an image file, and results in a new file where all pixels have been classified according to the decision regions. The matrix includes unclassified areas where few, if any, pixels are expected to fall. Each region is designed by a different symbol so that the general locations of pixels falling in these areas can be traced. Because of its format and function, the classifier will be referred to as a look-up table classifier.

The final product of the classified AVHRR data consists of maps showing the areal distributions of three general cover types. Before discussing the classification maps and map accuracies, it is necessary to examine the techniques developed for extracting the data of interest from the imagery, determining areal estimates of the cover types, and for monitoring temporal changes in the cover types (e.g., flooding). Monitoring areal changes in cover types requires that the data be registered from one acquisiton to another. This is especially true with NOAA-n data because of severe image distortion. Consequently, a major effort was made to overcome these problems, and the following section is devoted to discussing the registration technique employed.

Channel 1
(% Reflectance)

Channel 2
(% Reflectance)

W = Water

S = Soil

A = Vegetation

Figure 3-1. Stepped line look-up table classifier.

4. IMAGE TO IMAGE REGISTRATION OF NOAA-n DATA

As mentioned earlier, the wide view angle (110.8^0) of the AVHRR scanners produces predictable but unequal ground pixel sizes. The finest resolution, and hense smallest ground pixels, (1.1 square km), occur at nadir (at the Earth's surface directly beneath the satellite). Conversely, the largest ground areas represented by pixels, (16.1 square km), are located at the extremities of the view angle. This means that a ground feature of fixed dimensions will be represented by many more pixels if it is located at or near nadir than if it occurs near the edges of the image. Comparison of the area of a cover type from one acquisition to another must either take ground pixel size into account, or must use a suitable means of registering image data from two or more acquisitions. For the purposes of this study, the latter method was chosen, where an effective pseudo-registration technique was employed.

The registration technique described here enables one to compare the area of any large surface feature (e.g., a water body at least one square kilometer in width and breadth) from one acquisition to another. This method is based upon a grid system which has been superimposed over the Earth using a polar stereographic projection as its base. The grid cells are approximately 25 miles square, though this dimension varies a bit between the equator and the poles. The grid cells are designated by I, J coordinates where, in the northern hemisphere, the I values increase from west to east, and the J values increase from north to south. This grid will be referred to as the I, J Grid System, and was used here to register NOAA-6 AVHRR data on a grid cell basis.

The registration procedure involved identifying the I, J grid cells that fell over the area of interest (e.g., along a river to be monitored). This information was acquired from small-scale maps (smaller than 1:10,000,000) showing the location of grid line intersections. The intersections are numbered, and they represent the upper left corner of each cell (in the northern hemispehre only). Having identified the proper cells, their precise latitude and longitude locations were retrieved from a computer program called LLTOIJ. These coordinates were plotted carefully on base maps at a scale of 1:1,000,000 so that the locations of each cell were drawn clearly over the areas to be monitored. Next, computer compatible tapes containing NOAA-6 Local Area Coverage (LAC) data were obtained for the areas to be monitored. These were displayed on IMDACS, the interactive image data analysis system mentioned above. The color composites were screened for quality and cloud conditions, and a subjective analysis was performed on the areas of interest. This included general interpretations of land cover, and visual areal estimations including counting pixels considered to represent water bodies. These served for later comparison with classification results.

Having selected a usable set of image data over the area of interest, the LAC tapes (containing the original raw digital counts were submitted to a computer program called LACREG2. This program is the key to the registration technique because it separates the pixels from the image data file into individual files by I, J cell. Briefly, the user must specify which I, J cells cover the area of interest. The cell numbers are entered into the LACREG2 program which then computes all pixel locations with respect to the I, J Grid System. Those pixels falling into areas occupied by the designated I, J cells are put into separate files. These new files contain the digital counts for every pixel in each AVHRR channel, and they also retain the spatial arrangement between all pixels as they occur on the imagery. The latter feature is necessary for generation of the classification maps. The output from this program is simply a listing of the number of pixels grouped into each I-J cell and the new file name for each cell. Pixels extracted from one acquisition by LACREG2 and stored in a given set of I, J cell files cover basically the same areas on the Earth's surface as do pixels from other LACREG2 extractions from different acquisitions using the same set of I,J cells. While the number of pixels falling into a given cell will change significantly from one image set to another (as pixel sizes vary), the data is always registered to the same 25 mile square plot of ground. The spectral and spatial characteristics of the AVHRR data could then be compared by an I, J cell basis. Further, this registration technique is conducive to area estimation of Earth surface features since they can now be measured in terms of a percent of the known area of a cell.

The I, J cell files were also in a format suitable for the last stage: pixel classification and pixel mapping.

5. CLASSIFICATION AND MAPPING RESULTS

The look-up table classifier described in section 3 is part of a program called MAP1 which was developed for the present study. MAP1 reads the I, J cell files created by LACREG2 and classifies the pixels using the look-up table classifier. Finally, it prints the classified pixels from each I, J cell onto a CRT or line printer, preserving their spatial relationships (i.e., a map). The inputs to MAP1 are:

a) the name of the file containing the look-up table classifier,

b) the name of the file (or device) to which the output record is sent,

c) the name of the LACREG2 data file containing the spectral values from the desired image acquisition, and

d) the coordinates of the desired I, J cells.

The outputs include the map of classified pixels (about 25 miles square), the number of pixels in the cell, the file name, the pixel count for each category, and the percent area occupied by each category within the total map area.

An example of the MAP1 output is illustrated in Figure 5-1. The area shown covers most of Galveston Island, Texas and was chosen for testing the classifier. A comparison of the classified map with conventional maps of Galveston shows that the primary function of separating land from water performed quite well. The coastline and island shape is clearly in agreement with the actual coastal configuration. The cell area classified as land (soil and vegetation) compares well (within 5 percent) to the land area measured from the I,J cell plotted on a conventional map at 1:250,000. Problems were encountered in the separation of the soil and vegetation classes. Galveston Island was classisfied as having nearly total soil cover as the predominant surface feature. In reality, much of the island is covered by grasses, shrubs, and trees in the settled areas. However, it is likely that the soil background and dead leaf litter played a dominant role in the spectral return from the island. This shifted the pixel values into the soil-dominant decision region. Determination of an "optimum" soil/vegetation decision boundary would require considerable calibration with detailed ground truth, and even then, this "optimum" would probably not be applicable over large areas or at different times. The soil/vegetation distributions must be interpreted with care, since the decision boundaries were drawn on the basis of results from a wide range of ground conditions. Additional problems occurred between the cloud/soil classes. Some low cloud areas which cannot be visually discriminated were classified as soil. The cloud/soil threshold will require additional evaluation for improved results. Preliminary analysis indicates that the soil/cloud threshold (represented by "s" and "four" on the look-up table matrix) needs to be lowered by three to five reflectance counts in channel 1. The present study concentrated on perfecting the basic land/water discrimination for effective flood monitoring.

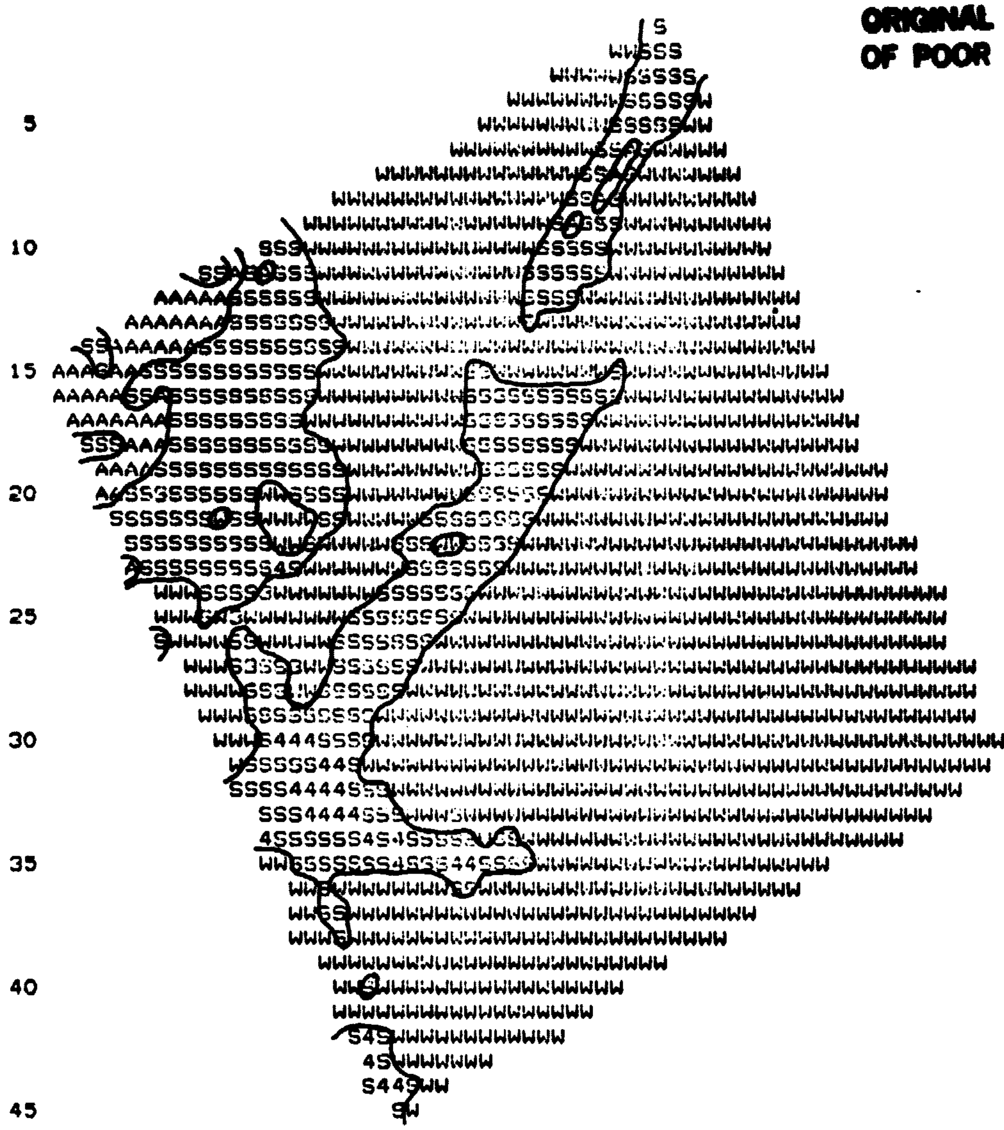

(I,J)=(219,398),
\# OF PIXELS= 1648

CHANNEL	SLOPE	INTERCEPT
2	0.10577E+00	-0.34539E+01
1	0.10709E+00	-0.41136E+01

FROM DATA FILE: [320,130]GT80237.DAT

TYPE,	COUNT,	PERCENT
W	1192	72.3301
A	52	3.1553
S	376	22.8155
1	0	0.0000
2	0	0.0000
3	4	0.2427
4	24	1.4563
5	0	0.0000
6	0	0.0000
7	0	0.0000
8	0	0.0000
9	0	0.0000

Figure 5-1. MAP1 classified map of Galveston Island, Texas

The look-up table classifier was tested over a number of different areas and acquisitions. Three additional I, J cells along the southeast Texas coast were classified using four separate acquisition dates: July 9, 1980; July 10, 1980 July 14, 1980; and August 14, 1980. These areas were ideal for testing the land/water discrimination capabilities because of the ease with which the results could be compared to existing coastal maps. In nearly every case, the water category differed by no more than 5 percent when comparing classification results between the four acquisitions.

In summary, the land/water discrimination capability worked very well for the Texas coast area, where both relatively clear ocean water and turbid bay waters occurred.

The final step was to test the classifier on an actual flood. The "Storm and Unusual Weather Phenomena" bulletin, published by NOAA, was consulted for reports on recent U.S. floods where some form of damage assessment had been made. Four areas of flooding were located in middle America during 1980. The floods were caused by localized severe thunderstorms and produced crop losses. Both black and white prints of channels 1 and 2, and tapes of AVHRR data were ordered from NOAA. The acquisition dates ranged from about two weeks before the floods to two weeks after the floods, and a total of nine dates were obtained. The prints were used primarily to locate the areas of interest and to determine whether cloud cover presented any problems. A large portion of the data set proved to be unusable due to cloud cover. The remaining scenes were displayed in false color on IMDACS for careful visual analysis of the areas in question. In each case, the acquisitions occurred either several days before the reported flooding, or three days to two weeks after the flooding. No indication of standing water was found on any of the post flood scenes, despite the fact that water bodies resolvable by the NOAA-n sensors were conspicuous on color composites of channels 1 and 2.

This was not surprising, since the rain occurred on land whose natural drainage system could likely handle most of the runoff after one to two days. By the time the clouds had dispersed, most of the surface flood water had disappeared. Futhermore, in all four areas the rains did not fall on flood plains were drainage would be slow. It was realized that the NOAA-n data would be more applicable to monitoring major floods occuring in areas of poor drainage such as flood plains with low gradients. These areas would be likely to have slower runoff rates, longer periods of inundation, and potentially cover larger areas.

Since no floods of this magnitude occurred in 1980-1981 in the U.S., a search was made for recent floods occurring in foreign areas. A major flood was located along the Parana River of Argentina where large areas of the flood plains were inundated. Satellite coverage of the flooded area was remarkably cloud-free on all three available acquisitions. The dates of coverage were: March 14, 1980; April 15, 1980; and February 20, 1981. The second date represents low to normal water levels in the river channel. The first and last dates were obtained during high water stages, where the river had overflowed its banks.

The analysis of the Parana River flood began with color composite displays of the LAC tape data. A major section of the river between 27° south latitude and 30° south latitude was chosen for detailed analysis. First twelve I, J cells were identified over the flood plain and were plotted onto a base map at 1:1,000,000. The I, J cell coordinates were then submitted to LACREG2 for pixel extraction from the three LAC tapes. When the cell files had been created by LACREG2, the MAP1 program was run, producing classified I, J cell maps for the three acquisitions much like Figure 5-1. Each I, J cell map was joined to its proper neighbor producing a mosaic of the entire river segment. A reduced, modified version of the three river mosaics is presented in Figure 5-2. Note that the percent water changed drastically from one acquisition to another. This is due primarily to the contrasts between the high water and low water stages. These classification results compare favorably to visual analysis of the color composite images, where pixel-by-pixel comparisons were made. However, a severe misclassification occurred with the April 15 data set in which water within the river channel at a low water stage was classified as soil. An analysis of the color image display shows that the river water is highly turbid and is characterized by relatively high reflectance in channel 1 (11-13 percent), and unusually high reflectance in channel 2 (11-15 percent). These characteristics put the water returns into the soil category. A scatterplot from this data set shows two clusters falling into the soil category. Further analysis is needed to determine if these actually represent the distinct land cover types of soil and water. If such is the case, the decision boundaries should be modified to reflect the unique spectral qualities of the April 15 data set.

Classification accuracies are difficult to determine without adequate ground truth. Pixels dominated by water are generally conspicuous on false color composites of NOAA-n data, and this has been substantiated by detailed comparison with base maps of 1:1,000,000 or larger where water bodies are clearly delineated. This has been further supported by comparison with Landsat color composites. Lacking ground truth, the classifications of the Parana River were compared with visual anlayses of color composite displays.

As mentioned above, severe misclassification occurred on the April 15 data. The other two dates produced much better results. However, the same problem occurred to a lesser degree, where water/soil pixels were indistinguishable when the Parana river°s continuity was interrupted by soil pixels (see the March 14 mosaic). The base maps and Landsat images were examined to assess the discontinuity of the river. The river was at its lowest water stage over two to three kilometers wide and the problem in classification was attributed to lack of distinction between turbid water and dark soils.

A second type of confusion occurred between wet soils and water. This distinction proved to be very difficult to make, even visually. Without ground truth, meaningful accuracy figures for the wet soil/water classes cannot be given. The wet soil/water classes shown in the I, J maps must be interpreted with care, and further analysis is needed to clarify these distinctions using areas for which ground truth data exists.

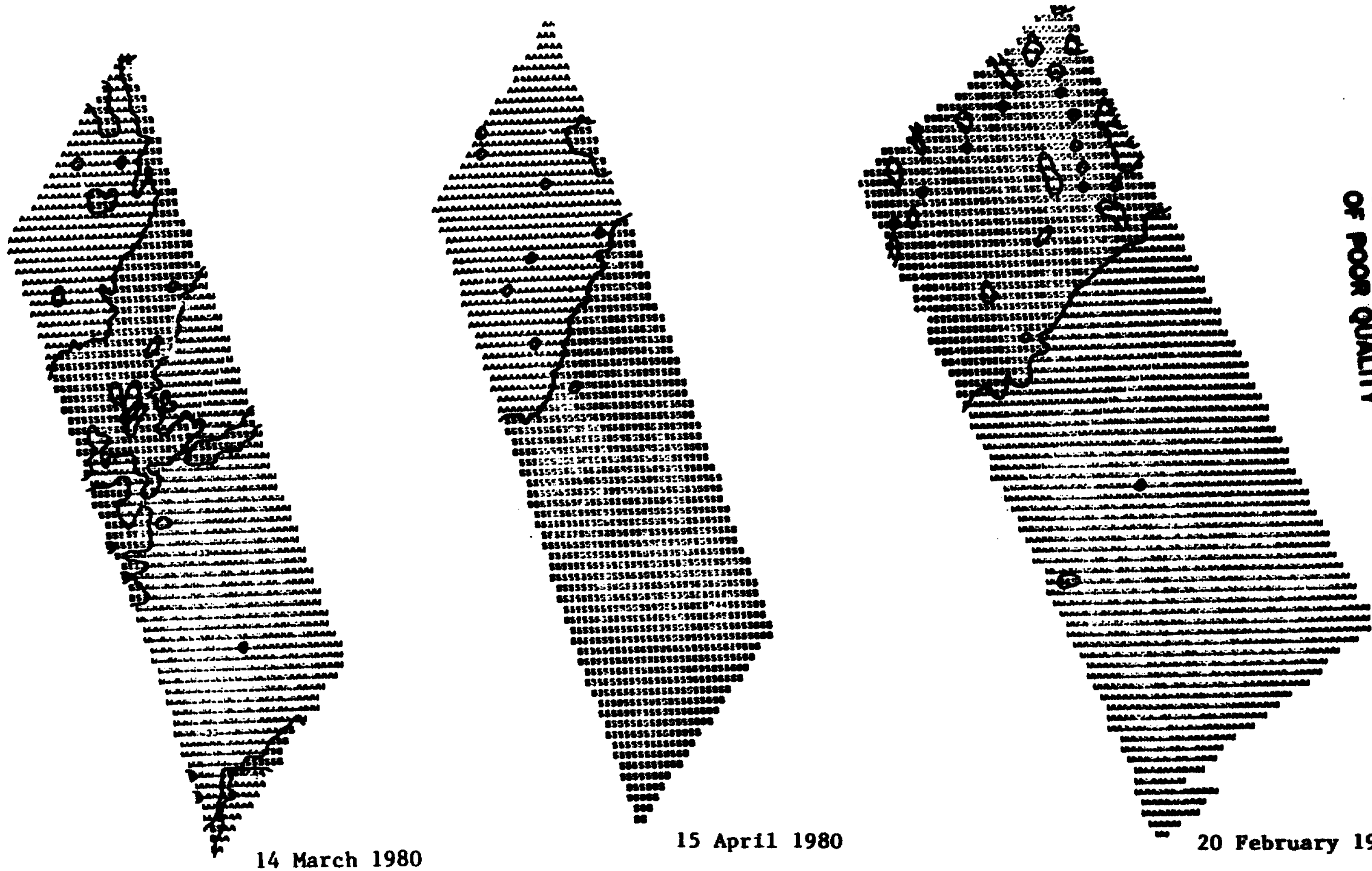

Figure 5-2. Three mosaics of the Parana River in Argentina showing low and high water levels.

Analysis was also performed on the spatial accuracies of the areas extracted by LACREG2. For comparisons between the percent water area of an I, J cell using two or more acquisitions, it is crucial that the pixels within the I, J cell represent the same 25 x 25 mile area on the Earth. However, some spatial variation does exist between the areas represented by pixels in an I, J cell. To measure this variation, prominent land features which appear repeatedly in all I. J cell classifications were located. Then, the distance between the I, J cell boundaries and these prominent features were measured. Since I, J cells do not have a uniform size when printed as classified maps (due to varying pixel size), distance was measured in tenths of the lengths and widths of the printed I, J cells. This unit allowed for a standardized comparison between I, J cells of different dimensions.

Seven different distance measurements were made for each of the four I, J classification maps of the Texas coastline. In every case, the x and y spatial variation between different acquisitions of a given I, J varied by no more than one twentieth of the side of a cell. This translates to no more than a 1 1/4 mile variation, or between one and two pixels at nadir.

The three Argentina acquisitions were compared in the same fashion. Two of the three acquisitions (February 20, 1981 and April 15, 1980) produced similar results, with spatial variation not exceeding 1 1/4 miles along both axes. The third date (March 14, 1980) varied significantly from the others: less than 1/14 miles in the x-direction, but 7 1/2 miles in the y-direction. This extreme shift has been known to occur occasionally in other LACREG2 extractions. Briefly, it is a function of a discrepancy between the predicted orbital position of the satellite (the number used in the image data header), and the actual position of the satellite. The pixels become registered to increasingly erroneous latitude and longitude coordinates until adjustments are made to reflect the actual satellite position. When this magnitude of spatial variation occurs along the y-axis, areal estimates of cover types should account for this before comparisons are made between acquisitions.

6. CONCLUSIONS

Much preliminary work has been realized in the use of NOAA-n data as a tool for land/water discrimination and flood monitoring. A basic understanding of the spectral returns in AVHRR channels 1 and 2 for water, soil, and vegetation has been gained. A simple classification system was developed upon which further research and refinement can be made. Furthermore, an effective method of image registration was employed which permits multi-temporal registration of NOAA-n data.

Several classification problems were encountered, but preliminary anlaysis indicated that these could be overcome by better ground truth support and more extensive analysis of the spectral scatterplots. The spatial registration worked well in most data sets, though significant misregistration in the y-direction was found in one case.

The present study was confined to examination of the reflective AVHRR channels. The less understood thermal channels may improve classification results when combined with the reflective channels. Clearly, much groundwork is needed for better understanding their contribution to measurements of environmental phenomena.